Nuclear Engineering and Technology 52 (2020) 734–741

Contents lists available at ScienceDirect

Nuclear Engineering and Technology

journal homepage: www.elsevier.com/locate/net

Original Article

Design of air-cooled waste heat removal system with string type direct contact heat exchanger and investigation of oil film instability

Jangsik Moon [a], Yong Hoon Jeong [a, *], Yacine Addad [b]

[a] Korea Advanced Institute of Science and Technology, 291 Daehak-ro, Yuseong-gu, South Korea
[b] Khalifa University of Science and Technology, 127788, Abu Dhabi, United Arab Emirates

ARTICLE INFO

Article history:
Received 29 March 2019
Received in revised form
1 October 2019
Accepted 14 October 2019
Available online 17 October 2019

Keywords:
Air cooling system
Rayleigh-plateau instability
Direct contact heat exchanger
Waste heat removal system

ABSTRACT

A new air-cooled waste heat removal system with a direct contact heat exchanger was designed for SMRs requiring 200 MW of waste heat removal. Conventional air-cooled systems use fin structure causing high thermal resistance; therefore, a large cooling tower is required. The new design replaces the fin structure with a vertical string type direct contact heat exchanger which has the most effective performance among tested heat exchangers in a previous study. The design results showed that the new system requires a cooling tower 50% smaller than that of the conventional system. However, droplet formation on a falling film along a string caused by Rayleigh-Plateau instability decreases heat removal performance of the new system. Analysis of Rayleigh-Plateau instability considering drag force on the falling film surface was developed. The analysis results showed that the instability can be prevented by providing thick string. The instability is prevented when the string radius exceeds the capillary length of liquid by a factor of 0.257 under stagnant air and 0.260 under 5 m/s air velocity.

1. Introduction

Currently, air cooling systems for the nuclear power plants are gaining attention. Advantages of air cooling systems are unlimited operation time, prevention of heat sink loss, and easier power plant siting in arid areas. In particular, air cooling systems are required in Small Modular Reactors (SMRs) which have been developed to provide distributed power source in order to compete with conventional thermal power plants. According to SPX Cooling Technologies, Inc. reports, different designs of thermal power plants are built in inland area and have air cooling systems for waste heat removal, in which 40% of the total air cooling systems are in China and 14% are located in Africa and Middle East [1]. These regions show growth of nuclear power generation and subsequently aim to replace aged thermal power plants with SMRs.

In general, air cooling systems are designed to be passive decay heat removal systems in many types of nuclear power plants [2–5]. However, research related to use of air cooling systems as waste heat removal systems has not been widely studied. Large-sized air cooling systems have to be designed due to the low conductivity and density of air. In particular, waste heat removal systems require large surface area for a heat exchange, where the temperature difference between the heat sink and the condenser is designed to be small in order to obtain a high cycle efficiency. Conventional air cooling systems utilize a fin structure for getting large surface area. However, such structure requires volume and weight, in addition, high thermal resistance of the systems due to conduction resistance of the fins occurs and leads to low heat transfer performance [6].

Using a direct contact heat exchanger, which does not require a physical wall between hot and cold fluids, is one of the options to replace the fin structure in the air cooling systems [7]. In addition, the direct contact heat exchanger has simpler structure and higher heat transfer performance compared to the fin structure. However, one of the considerable problems of the heat exchanger is vaporization of the liquid. Therefore, fluids with low vapor pressures, such as mineral oils and silicone oils, are recommended.

Currently, developing more compact direct contact heat transfer technology is the main focus of the nuclear industry. Several conceptual designs of the air cooling waste heat removal systems equipped with direct contact heat exchanger have been introduced. Researchers from UCLA, Zeng et al., developed the Direct-Contact Liquid-on-String Heat Exchanger (DILSHE) where liquid flows on the strings as shown in Fig. 1a. Therefore, direct contact heat transfer occurs on the liquid's surface [8]. A Spray Freezing of

* Corresponding author.
E-mail address: jeongyh@kaist.ac.kr (Y.H. Jeong).

https://doi.org/10.1016/j.net.2019.10.010

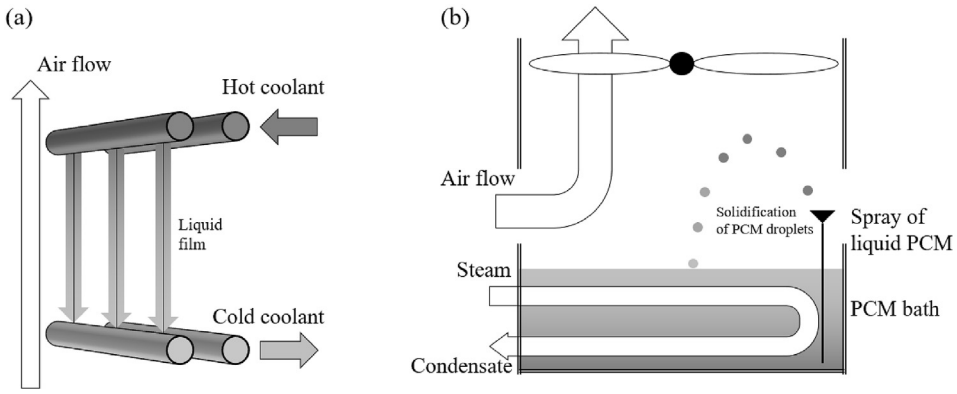

Fig. 1. Diagram a) shows the concept behind DILSHE [8] and b) the operating description of a Spray Freezing of Recirculating PCM system [9].

Recirculating Phase Change Material (PCM) system was developed at Drexel University, Shabgard et al. In this system, spherical droplets of the PCM are sprayed into the air as shown in Fig. 1b [9].

A previous study about heat transfer performance per unit pressure drop of air in various types of direct contact heat exchangers showed that a direct contact heat exchanger using vertical strings is the most effective. Air in vertical string type direct contact heat exchanger has heat transfer performance per unit pressure drop 1.5–2 times as high as that of air in horizontal string type and droplet type direct contact heat exchangers [10].

However, two kinds of instabilities might occur in the falling film along the vertical string. The first one is called Rayleigh-Plateau instability, where droplets are formed from the falling film due to surface tension [11]. When the falling film of the vertical string type direct contact heat exchanger becomes droplets due to the mechanism of Rayleigh-Plateau instability, the heat exchanger has heat transfer performance per unit pressure drop 0.5–0.7 times that of the heat exchanger with straight film forming on vertical strings [10]. The second instability is characterized by the falling film forming a small wavy surface due to inertia and is known as the Kapitza instability [12]. However, the small wave of liquid film by Kapitza instability induces similar heat transfer performance per unit pressure drop on air as that of with a straight film [13]. Therefore, the primary focus should be on the prevention of the Rayleigh-Plateau instability in order to design an effective direct contact heat exchanger.

The Rayleigh-Plateau instability has been widely studied. Quéré revealed that the instability does not occur at large fiber coated with a thin film and defined conditions for prevention of the instability for very thin film and string [14]. Kliakhandler et al. theoretically and experimentally analyzed a thick liquid film along a string [15]. Duprat et al. obtained a flow regime map for a liquid film along a vertical string with stagnant air. The flow regime is determined by the film thickness, liquid viscosity, and string thickness [16].

These studies were conducted with stagnant air condition; therefore, a drag force on surface of the liquid film has been neglected. In case of the direct contact heat exchanger, the drag force by counter-current air flow on the liquid film needs to be evaluated. Several studies observed a droplet formation of liquid film on a vertical string under a counter-current air flow. Zeng et al. discovered that the air velocity increases with the size of the droplet, while Grunig et al. studied how the counter-current flow affects the breakup of the falling film [8,17]. However, conditions for prevention of the Rayleigh-Plateau instability have not been evaluated.

In this study, physical modeling and experiments on prevention of the Rayleigh-Plateau instability were executed. In addition, design of a new waste heat removal system with direct contact heat exchanger is introduced. The new system was designed for application in SMRs such as SMART, requiring 200 MW heat removal performance.

2. Design of the system

2.1. Purpose and method

The concept of the new waste heat removal system with vertical string type direct contact heat exchanger is shown in Fig. 2. Steam from turbine condenses in a fin tube heat exchanger submerged in an oil pool and resulting condensate returns to steam generators. A pump makes heated oil flow to thin vertical strings. The oil returns to the oil pool by gravity while air flows along a cooling tower. Silicone oil-100 cst, which has low vapor pressure (less than 0.1 mmHg at 300 K), fills the oil pool. The oil is not lost during the operation due to its non-evaporative property. In addition, the flash point of the oil (315 °C) is sufficiently higher than temperature of

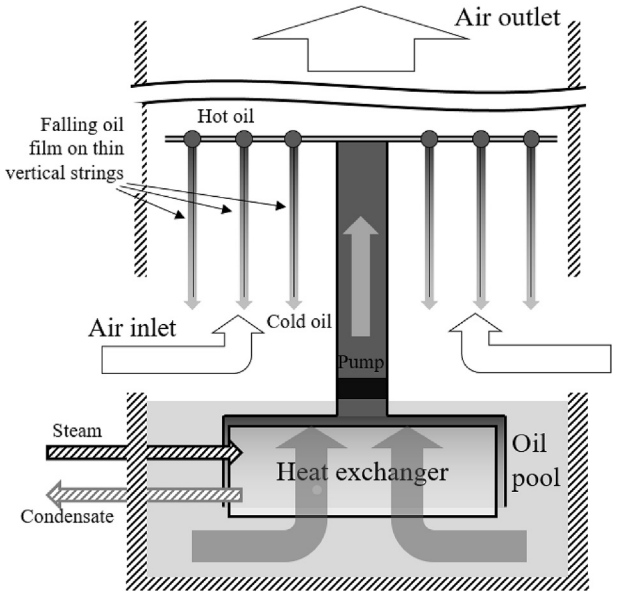

Fig. 2. Design concept of the new waste heat removal system.

the steam from turbine (~40 °C) and the highest temperature of the secondary side of the nuclear power plants (285 °C) [18].

The goal of the new system is to remove 200 MW of waste heat, which is approximately the amount of waste heat in SMRs. The new system was designed to have 200 MW heat removal performance at 10 K temperature difference between air and steam from turbine. This condition is same as in water-cooled condensers in the nuclear power plants; therefore, the system can maintain power cycle efficiency of the nuclear power plants. Air temperature is assumed to be 30 °C, then steam from turbine temperature is 40 °C.

In this study, both the conventional ACC and the new systems were analyzed. The conventional ACC with a fin tube heat exchanger, generally having geometric conditions as shown in Fig. 3, was evaluated in previous study with conditions of steam temperature of 40 °C and air temperature of 30 °C [19]. The new system was analyzed by obtaining the following parameters: the size of the direct contact heat exchanger for 200 MW heat removal, pressure drop on air side of the direct contact heat exchanger, and the cooling tower height providing enough driving pressure.

The analysis was conducted by controlling the cooling tower footprint area. Vertical strings of the direct contact heat exchanger have 1.5 mm diameter and total cross-sectional area of the strings is 3% of the footprint area of the cooling tower. Oil is assumed to be distributed uniformly to the vertical strings.

2.2. Heat transfer performance

The heat is transferred from the steam to air through two heat exchangers connected in series: fin tube heat exchanger in the oil pool and direct contact heat exchanger in the cooling tower. Thermal resistance of the heat exchanger in the oil pool is very small compared to the direct contact heat exchanger. Therefore, the oil pool temperature is assumed to have small difference with the steam temperature as shown in Table 1, and only the direct contact heat exchanger was analyzed.

$$Q = \frac{\Delta T_{lm}}{R_1 + R_2}, R_1 = (h_d A_s)^{-1}, \quad R_2 = (h_a A_s)^{-1} \tag{1}$$

The direct contact heat exchanger is investigated by applying the conduction equation for oil film and convection correlation for air as listed in Table 2. Where Nu is Nusselt number, k_0 is thermal conductivity of oil, d_h is hydraulic diameter, r is string radius, δ is film thickness, Re is Reynolds number, Pr is Prandtl number and k_a is thermal conductivity of air. The heat transfer performance and thermal resistance of the direct contact heat exchanger were calculated as follows [20]:

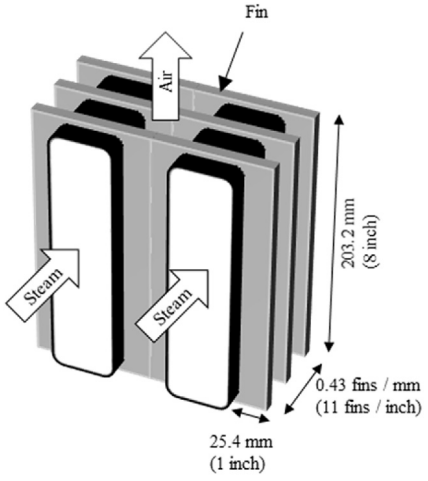

Fig. 3. Fin tube heat exchanger in conventional ACC.

Table 1
Steam and oil temperatures.

Parameters	Values
Steam temperature	40°C
Inlet oil temperature	37°C
Outlet oil temperature	39°C

Where Q is the heat transfer rate, ΔT_{lm} is the log mean temperature difference between air and oil, R_1 is the thermal resistance of liquid film, R_2 is the thermal resistance of air and A_s is the total surface area of liquid films. Thickness of falling film on vertical string is an important parameter to obtain the hydraulic diameter of the system.

$$d_h = \frac{4A_a}{2\pi(r+\delta)n} \tag{2}$$

$$\dot{m} = \frac{\pi\rho_o^2 g}{\mu_o}\left[\frac{1}{2}(r+\delta)^4 \ln\frac{r+\delta}{r} - \frac{1}{4}\left(2r\delta+\delta^2\right) - \frac{1}{8}\left\{(r+\delta)^4 - r^4\right\}\right] - C\frac{2\rho_o}{\pi}(r+\delta)\left[-2r\delta + 2(r+\delta)^2 \ln\frac{r+\delta}{r} - \delta^2\right] \tag{3}$$

Where A_a is the air flow area and n is the number of strings. The film thickness can be determined from mass flow rate of the film. The mass flow rate of the oil film on a string $\dot{m}$ is calculated as follows [21]:

Where ρ_o is the density of oil, g is the gravitational acceleration (9.81 m^2/s), μ_o is the viscosity of oil, and C is defined by the following equation:

$$C = \frac{f\rho_a v_r^2}{8\mu_o} \tag{4}$$

Where f is the Darcy friction factor, ρ_a is the density of air, and v_r is the relative velocity of air. The mass flow rate of oil is considered to be a design parameter; therefore, the thickness of the film can be obtained and Eq. (1) can be solved.

2.3. Pressure drops in cooling tower

Fig. 4 shows pressures in the cooling tower. Atmospheric pressure at the top of the cooling tower P_2 is equal to outlet air pressure of the cooling tower P_4. The pressures can be obtained by the Barometric formula as follows [22]:

$$P_2 = P_1 \exp\left[\frac{-gMH}{RT_1}\right], P_4 = P_3 \exp\left[\frac{-gM(H-L)}{RT_3}\right] \tag{5}$$

Table 2
Correlations for the heat transfer coefficients.

Heat transfer coefficients	Correlations
Conduction in oil film	$h_d = \frac{k_o}{(r+\delta)\ln\left(\frac{r+\delta}{r}\right)}$
Convection of air	$h_a = \mathrm{Nu}\frac{k_a}{d_h} = 0.023\mathrm{Re}^{0.8}\mathrm{Pr}^{0.3}\frac{k_a}{d_h}$

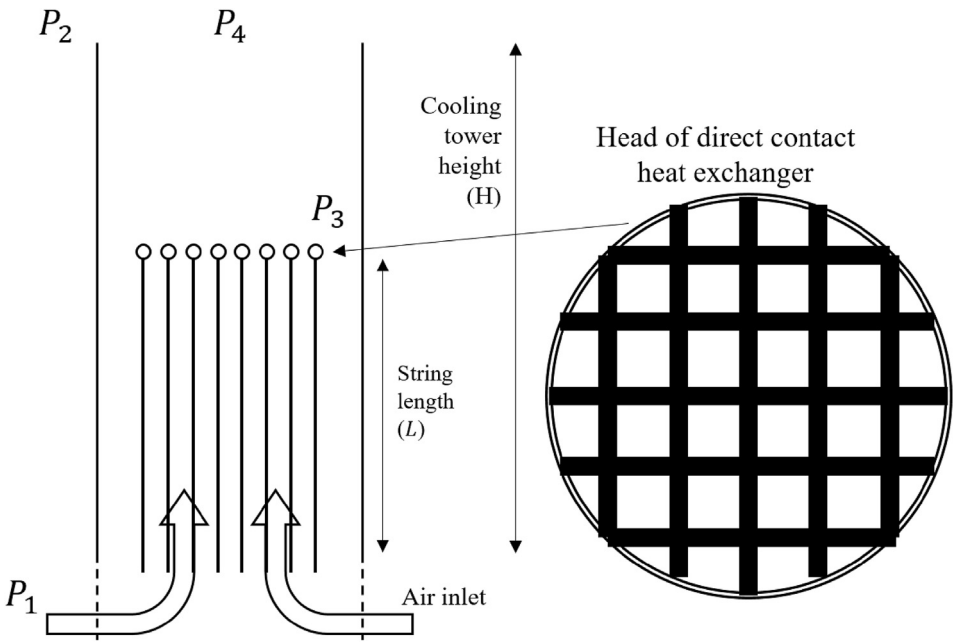

Fig. 4. Pressures in the cooling tower.

Where, M is the molar number of air, H is the height of the cooling tower, L is the length of the string, R is the gas constant, P_1 is the inlet air pressure, T_1 is the inlet air temperature, P_3 is the pressure at the top of the direct contact heat exchanger and T_3 is the outlet air temperature. The height of the cooling tower is obtained from Eq. (5) as follows:

$$H = \frac{1}{T_3 - T_1}\left[\frac{T_1 T_3 R}{gM}\ln\left(\frac{P_1}{P_3}\right) - T_1 L\right] \tag{6}$$

P_3 is calculated by P_1 and pressure drops as follows:

$$P_3 = P_1 - \Delta P_f - \Delta P_g \tag{7}$$

Where ΔP_f is the frictional pressure drop and ΔP_g is the gravitational pressure drop. The frictional pressure drop is calculated by the Blasius equation and the gravitational pressure drop is calculated by average density of air in the direct contact heat exchanger as follows, respectively [18]:

$$\Delta P_f = f\frac{L}{d_h}\frac{\rho_a v_r^2}{2}, \quad \text{for } f = 0.316\mathrm{Re}^{-0.25} \tag{8}$$

$$\Delta P_g = \rho_a g L \tag{9}$$

2.4. Minimum height of cooling tower

At a specific footprint area of the cooling tower, cooling tower height is minimized when the pressure drop is minimized. The Darcy friction factor is derived from the Chilton-Colburn analogy, which explains the relation between pressure drop and heat transfer performance [7].

$$f = 8(\mathrm{Nu})(\mathrm{Re})^{-1}(\mathrm{Pr})^{-1/3} = 8\frac{\mu_a h_a}{\rho_a v_r k_a}\mathrm{Pr}^{-1/3} \tag{10}$$

The pressure drop and heat transfer coefficient are expressed respectively by the following equations:

$$\Delta P_f = f\frac{L}{d_h}\frac{\rho_a v_r^2}{2} \cong f\frac{A_s}{A_a}\frac{\rho_a v_a^2}{8}, \quad h_a = \mathrm{Nu}\frac{k_a}{d_h} \tag{11}$$

Where v_a is the air velocity. The surface area is calculated by the heat removal performance and the temperature difference between air and the falling oil. Therefore, the pressure drop is further derived as follows:

$$\Delta P_f = f\frac{Q}{h_a \Delta T_{lm} A_a}\frac{\rho_a v_a^2}{8}, \quad A_s = \frac{Q}{h_a \Delta T_{lm}} \tag{12}$$

From Eqs. (9) and (11), final expression for pressure drop is obtained as:

$$\Delta P_f = \frac{\mu_a}{\rho_a k_a \mathrm{Pr}^{-1/3}}\frac{Q}{A_a^2}\frac{\dot{m}_a}{\Delta T_{lm}} \tag{13}$$

Where $\dot{m}_a$ is mass flow rate of air. Eq. (13) shows that the pressure drop is proportional to a function $\dot{m}/\Delta T_{lm}$. Fig. 5 shows a relation between outlet air temperature and the function with inlet air temperature being 30 °C. The function is minimized when the outlet air temperature is 36 °C. Therefore, the system is designed to have outlet air temperature of 36 °C.

2.5. Results of system analysis

Both new and conventional systems were analyzed by a developed code in Matlab and the results show that the new system requires smaller cooling tower than conventional system due to high heat transfer performance per unit pressure drops. Fig. 6 shows height and diameter of the cooling tower for 200 MW heat removal.

Fin structure of the conventional system takes large volume in the cooling tower and that leads to decrease of air flow area and increase of frictional pressure drop. Fig. 7 shows that about 45% of cooling tower area are covered by fin structures, while films and strings of the new system cover only 10%. Moreover, thermal

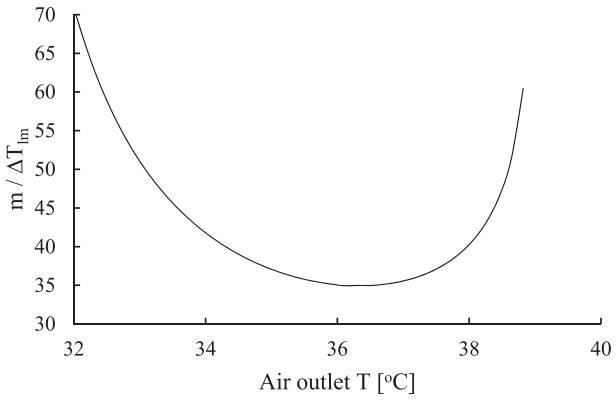

Fig. 5. Relation between outlet air temperature and function with inlet air temperature being 30 °C.

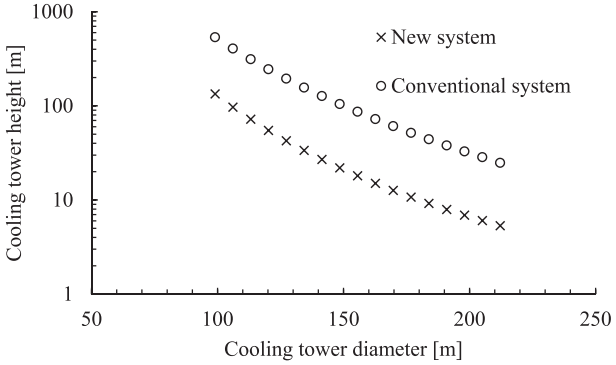

Fig. 6. Cooling tower height for 200 MW waste heat removal.

resistance of the conduction in the fin structures decreases the heat transfer performance of the conventional system and fin efficiency was calculated to be 0.55. The new system has thermal resistance caused by the conduction in film flowing down along the vertical string. However, the thermal resistance was found to be only 10–30% of the total thermal resistance of the system as shown in Fig. 8. Both of the systems have similar thermal resistance of air, but large air flow area and small thermal resistance of oil film provides high heat removal performance of the new system.

3. Prevention of Rayleigh-Plateau instability

3.1. Physical modeling

Duprat et al. created a Rayleigh-Plateau instability map while considering surface tension, viscous force, and gravity on a film flowing down along a vertical string [17]. The Rayleigh-Plateau instability was observed to occur when the film thickness becomes within specific range as shown in Fig. 9. Duprat et al. revealed that the Rayleigh-Plateau instability does not happen when string radius is 0.24 times the capillary length of the oil.

However, because the new system employs counter-current air flow on the oil film surface, region of the Rayleigh-Plateau instability changes. This analysis is based on spatio-temporal analysis [23]. Fig. 10 shows oil film on a vertical string. The oil film thickness is expressed by the following equation:

$$\delta = \delta_0 + \delta_1 f(z,t) = \delta_0 + \delta_1 \exp[i(kz - wt)] \tag{14}$$

The wave function consists of spatial part and temporal part, where k is the wave number, z is the axial location, w is the period of the wave and t is the time. Both k and w are complex numbers and Eq. (16) can be written as:

$$f(z,t) = \exp[-k_i z + w_i t + i(k_r z - w_r t)] \tag{15}$$

Where k_i and w_i are the imaginary parts and k_r and w_r are the real parts of the k and w. The w_i describes the magnitude of instability on the film during time. The film is stable when the largest w_i is less than zero. Such case is called convective instability. Contrarily, when the variable is greater than zero, the instability is amplified and is called absolute instability [23].

$$\begin{aligned} &w_i(k_0) < 0, \text{convective instabilty (globally stable)} \\ &w_i(k_0) = 0, \text{threshold of absolute instability} \end{aligned} \tag{16}$$

The k_0 is the value of k making the largest value of w_i. It is obtained by the following conditions:

$$\frac{\partial w_i}{\partial k_i}(k_0) = \frac{\partial w_i}{\partial k_r}(k_0) = 0 \tag{17}$$

In order to find the wave function on the falling film along vertical string, the following relations construct the momentum balance on the falling film [24]:

$$\rho_0 g - \partial_z p + \frac{\mu_o}{y}\partial_y(y\partial_y u) = 0 \tag{18}$$

$$u(r) = 0, \quad \partial_y u|y = r + \delta = \tau \Big/ \mu_o = C = \frac{f\rho_a v_r^2}{8\mu_o} \tag{19}$$

Where $\partial_z p$ is the pressure gradient caused by surface tension, $u(y)$ is the flow velocity in vertically downward axis z for specific value in radial direction axis y, τ is the sheer stress on liquid film surface.

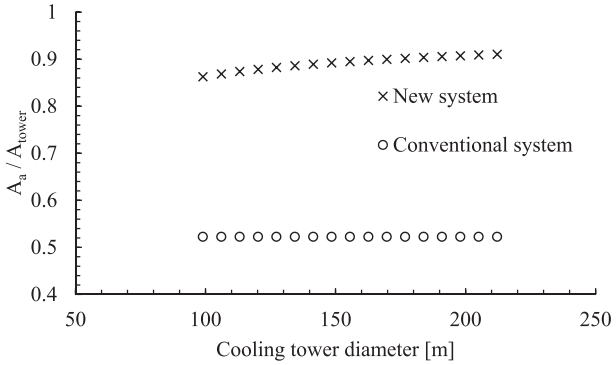

Fig. 7. Effective air flow area in cooling tower.

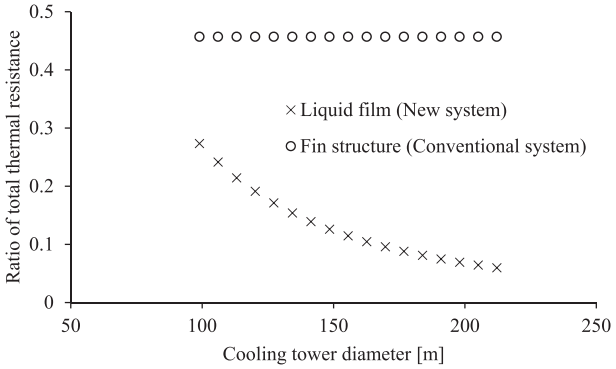

Fig. 8. Ratio of total thermal resistance.

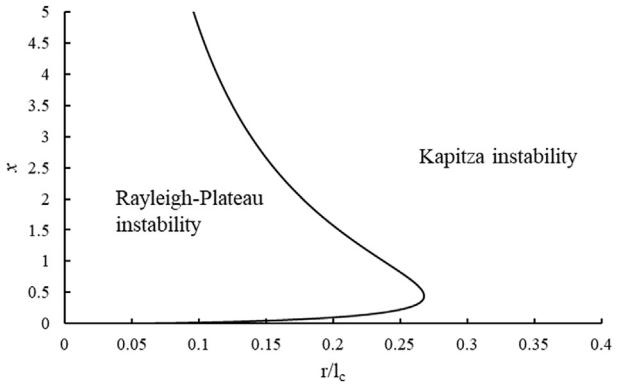

Fig. 9. Instability map of a film flowing down along vertical string [12].

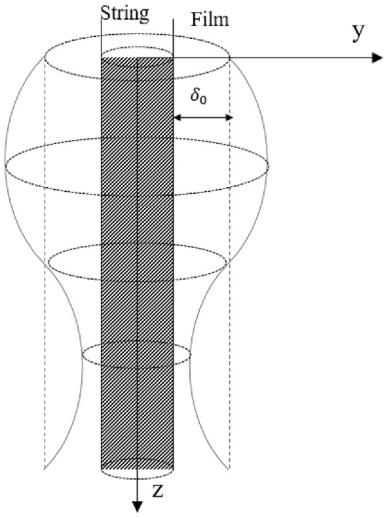

Fig. 10. Oil film on vertical string.

The flow velocity is expressed as follows:

$$u(y)=\frac{\partial_z p-\rho_o g}{2\mu_o}\left[(r+\delta)^2\ln\left(1+\frac{y}{r}\right)-\frac{y(2r+y)}{2}\right]+C(r+\delta)\ln\left(1+\frac{y}{r}\right) \tag{20}$$

Laplace's law calculates the pressure gradient as [24]:

$$\partial_z p=-\sigma\left[\frac{1}{(r+\delta)^2}\partial_z\delta+\partial_{zzz}\delta\right] \tag{21}$$

Where σ is the surface tension of oil. The falling film is considered to be an incompressible fluid. Therefore, the following relations are based on the mass balance [24]:

$$\partial_t\delta+\partial_z q=0 \tag{22}$$

$$q=\frac{1}{(r+\delta)}\int_0^{\delta}(r+y)u(y)\mathrm{d}y=\frac{\partial_z p-\rho_o g}{2\mu_o(r+\delta)}\delta^4 B(x)+\frac{C}{4}\delta^2 D(x) \tag{23}$$

$$B(x)=\frac{1}{x^4}\left[\frac{(1+x)^4\ln(1+x)}{2}-\frac{x^2(2+x)^2}{4}-\frac{(1+x)^4-1}{8}\right] \tag{24}$$

$$D(x)=\frac{1}{x^2}\left[-2x+2(1+x)^2\ln(1+x)-x^2\right] \tag{25}$$

Where q is the flow rate per unit length, x is δ/r, and $B(x)$ with $D(x)$ are form factors. Finally, the w is derived as:

$$w=k\left[\frac{\rho_o g\delta_0^2}{2\mu_o}\frac{x(4+3x)}{(1+x)^2}B(x)-\frac{C\delta_0}{2}D(x)\right]+i\frac{\sigma\delta_0^3}{3\mu_o(r+\delta_0)^4}\frac{3x}{2(1+x)}B(x)\left[k^2(r+\delta_0)^2-k^4(r+\delta_0)^4\right] \tag{26}$$

3.2. Prevention of Rayleigh-Plateau instability

The complicated Eq. (27) can be simplified by substitution of variables as follows:

$$w=E(x)\left[KU+i\left(K^2-K^4\right)\right],\quad K=k(r+\delta_0) \tag{27}$$

$$U=\frac{r^2}{l_c^2}\frac{(1+x)^2(4+3x)}{x}-C\frac{\mu_o r}{\sigma}\frac{(1+x)^3}{x^2}\frac{D(x)}{B(x)} \tag{28}$$

Where $E(x)$ is a form factor and l_c is the capillary length of oil. Elements w and K both consist of a real part and an imaginary part. When the largest w_i is smaller than 0, the Rayleigh-Plateau instability is prevented. From Eqs. (17) and (27), threshold condition U' is defined by following relations [23]:

$$U'=32\left(\frac{7^{1/2}-1}{24}\right)^{3/2}+4\left(\frac{7^{1/2}-1}{24}\right)^{1/2}=1.622 \tag{29}$$

For U greater than U', the instability becomes the convective instability and Rayleigh-Plateau instability is prevented. With this condition, an instability maps were obtained as shown in Figs. 11 and 12. The results show that the absolute instability can be avoided if the film thickness is very small or very high. In addition, the instability is not observed when the string radius is greater than that of 0.257 times the capillary length of the fluid. The absolute instability region expands with air flow velocity; however, Fig. 12 shows that the region increases to only 1% at the real system condition, which has air flow velocity of 3–5 m/s.

The studied system had strings of 1.5 mm diameter, which was 0.6 times the capillary length of silicone oil 100 cst; therefore, the Rayleigh-Plateau instability on the film flowing down on the strings was not observed.

3.3. Experimental apparatus

An experiment was conducted to observe a presence of the Rayleigh-plateau instability on the film along the vertical string. The experimental apparatus is shown in Fig. 13. A rubber string having 1.5 mm diameter was used and weight was installed at the tip of the string. An oil pool filled with silicone oil 100 cst was connected to a nozzle in an acryl tube having 25 mm inner diameter and 1500 mm length. The oil pool had small heater for maintaining oil temperature at 30 °C. An ejector was installed at top of

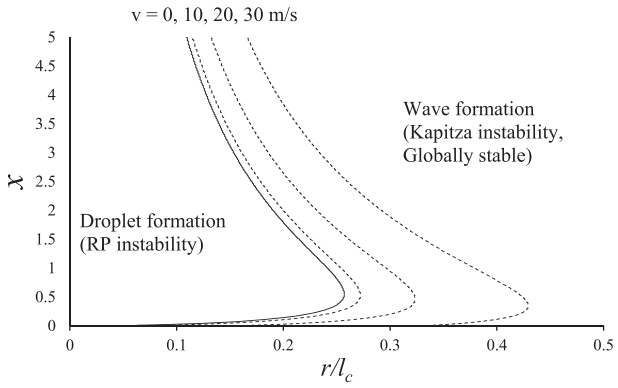

Fig. 11. Rayleigh-Plateau instability map under counter-current air flow (10–30 m/s).

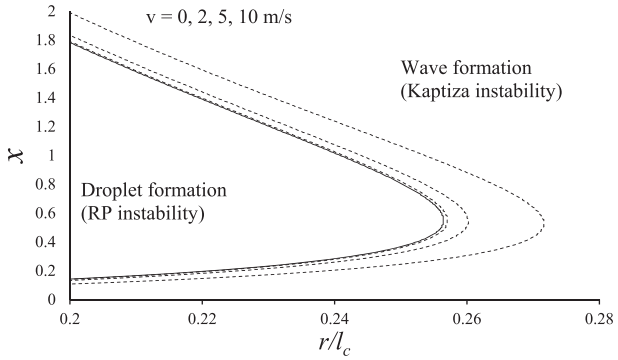

Fig. 12. Rayleigh-Plateau instability map under counter-current air flow (2–10 m/s).

the tube and was used to absorb 20 $^{\circ}C$ air in order to form homogeneous inlet airflow in the tube. The experimental apparatus had 23 mm hydraulic diameter and Reynolds number was kept similar with that of the real system with a value range of 4000–7000.

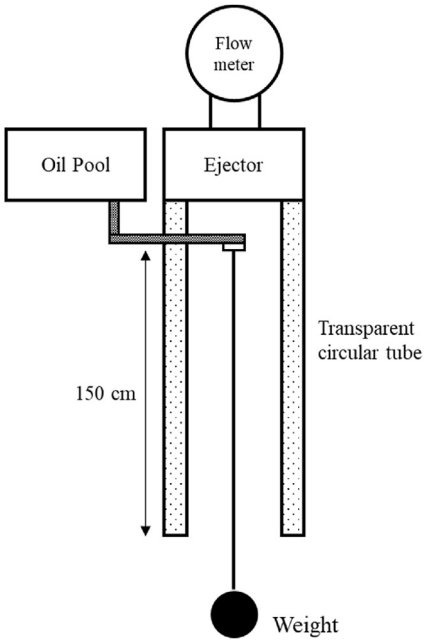

Fig. 13. Experimental apparatus.

The experiment was conducted under stagnant air and counter-current air flow. Air flow velocity was controlled from 1.5 m/s to 4.07 m/s to obtain desired values of Reynolds number. In the experiment condition, the instability map was obtained as Fig. 14. The nozzle was controlled to generate 0.13 g/s of oil mass flow. The oil film was observed by high-speed camera focused on 40 cm below the nozzle. The air flow rate was obtained by flow meter installed at the top of the acryl tube.

3.4. Observation of film formation on a vertical string

The Rayleigh-Plateau instability was not observed on film during the experiments for both cases of counter-current air flow and stagnant air. Film formation on vertical string in counter-current air flow is shown in Fig. 15. Only the Kapitza instability on the film was observed and the wave amplitude increases insignificantly with the air flow rate. The new system has 1.5 mm diameter strings and 3.5 m/s air flow; therefore, the film flows in globally stable condition and is not separated into series of droplets.

4. Conclusion

A new air-cooled waste heat removal system utilizing a direct contact heat exchanger was designed to have high heat transfer

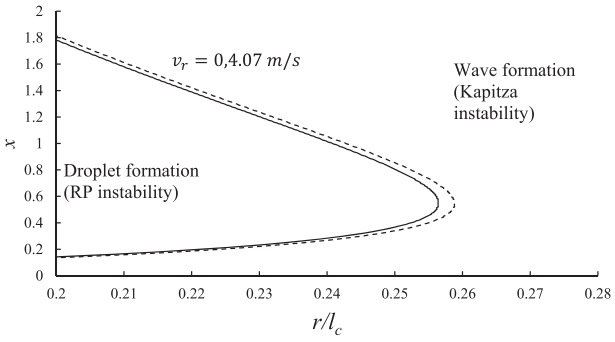

Fig. 14. Instability map with experiment condition.

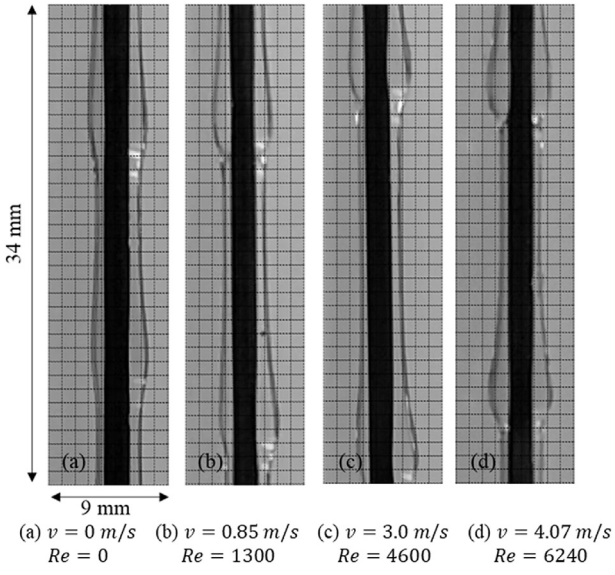

Fig. 15. Film formation on a vertical string in counter-current air flow.

performance. The new system has higher heat transfer performance per unit pressure loss than the conventional air cooling system; therefore, smaller cooling tower than that of the conventional system is required. The fin structure of the conventional system has high thermal resistance which is 50% of total thermal resistance of the system, whereas the oil film of the new system has conduction thermal resistance which is only 10–30% of total thermal resistance of the system. Moreover, the conventional system has small air flow area due to large volume of fin structures, while the new system has large air flow area due to the small volume of the direct contact heat exchanger.

This system has stable oil flow on vertical strings. Physical modeling considering viscous force, surface tension, gravity, and interfacial force on oil film surface due to counter-current air flow was conducted. The results showed that the effect of air flow on the oil film is small enough to be neglected. An instability map was obtained and the results show that the Rayleigh-Plateau instability does not occur on the film along the thick string. Experiments were conducted in the same condition with the new system and the instability was not observed.

In this experiment, 1.5 mm string diameter was used to observe Rayleigh-Plateau instability. The diameter was thick enough to prevent the instability. Therefore, the obtained instability map could not be verified through this experiment. The validity of the obtained instability map is to be the aim of future studies.

Acknowledgments

This work was supported by the KUSTAR-KAIST Institute, Republic of Korea, under the R&D program supervised by KAIST.

References

[1] Spx Dry Cooling Systems, A Leadership in Dry Cooling Technologies, 2017.
[2] Y. Zhang, S. Qiu, G. Su, W. Tian, Design and transient analyses of emergency passive residual heat removal system of CPR1000. Part I: air cooling condition, Prog. Nucl. Energy 53 (5) (2011) 471–479.
[3] X. Yan, H. Sato, Y. Inaba, H. Noguchi, Y. Tachibana, K. Kunitomi, Evaluation of GTHTR300A nuclear power plant design with dry cooling, Int. J. Energy Res. 38 (11) (2014) 1467–1477.
[4] G. Wu, M. Jin, J. Chen, Y. Bai, Y. Wu, Assessment of RVACS performance for small size lead-cooled fast reactor, Ann. Nucl. Energy 77 (2015) 310–317.
[5] G. Caruso, M. Fatone, A. Naviglio, An experimental study on natural draft-dry cooling tower as part of the passive system for the residual decay heat removal, in: Proceedings of ICAPP, July, 2007.
[6] H. Zhai, E.S. Rubin, Performance and cost of wet and dry cooling systems for pulverized coal power plants with and without carbon capture and storage, Energy Policy 38 (10) (2010) 5653–5660.
[7] G.F. Hewitt, G.L. Shires, T.R. Bott, Process Heat Transfer, FL, CRC press, Boca Raton, 1994.
[8] Z. Zeng, A. Sadeghpour, G. Warrier, Y.S. Ju, Experimental study of heat transfer between thin liquid films flowing down a vertical string in the Rayleigh-Plateau instability regime and a counter flowing gas stream, Int. J. Heat Mass Transf. 108 (2017) 830–840.
[9] H. Shabgard, H. Hu, M. Rahman, P. Boettcher, M. McCarthy, Y. Cho, Y. Sun, Indirect Dry Cooling of Power Plants Using Spray-Freezing of Phase Change Materials, 2015.
[10] J. Moon, Y.H. Jeong, Study on various direct contact heat exchanger types for dry cooled waste heat removal system in SMRs, in: Transactions of the Korea Nuclear Society Spring Meeting, May, 2018.
[11] L. Rayleigh, On the instability of jets, Proc. Lond. Math. Soc. 1 (1) (1878) 4–13.
[12] D. Ter, Haar, Collected Papers of PL Kapitza, Elsevier, 2016.
[13] Z. Zeng, A. Sadeghpour, Y.S. Ju, Thermohydraulic characteristics of a multi-string direct-contact heat exchanger, Int. J. Heat Mass Transf. 126 (2018) 536–544.
[14] D. Quéré, Thin films flowing on vertical fibers, Europhys. Lett. 13–8 (1990) 721.
[15] I.L. Kliakhandler, S.H. Davis, S.G. Bankoff, Viscous beads on vertical fibre, J. Fluid Mech. 429 (2001) 381–390.
[16] C. Duprat, C. Ruyer-Quil, F. Giorgiutti-Dauphiné, Spatial evolution of a film flowing down a fiber, Phys. Fluids 21 (4) (2009) 042109.
[17] J. Grünig, E. Lyagin, S. Horn, T. Skale, M. Kraume, Mass transfer characteristics of liquid films flowing down a vertical wire in a counter current gas flow, Chem. Eng. Sci. 69 (1) (2012) 329–339.
[18] Shin-etsu, Silicone fluid performance test results. http://www.shinetsusilicone-global.com/catalog/pdf/kf96_e.pdf retrieved fromhttps:.
[19] J. Moon, A.S. Alkaabi, Y.H. Jeong, Optimized design of residual heat removal system with dry cooling technology for the APR1400 design, in: The 11th International Topical Meeting on Nuclear Thermal-Hydraulics, Operation and Safety (NUTHOS-11), October, 2016.
[20] Y. Cengel, Heat and Mass Transfer: Fundamentals and Applications, McGraw-Hill Higher Education, 2014.
[21] J. Moon, Y.H. Jeong, Dry cooling system with direct contact heat transfer on the falling film along vertical straight string, in: Transactions of the Korea Nuclear Society Spring Meeting, May, 2017.
[22] M.N. Berberan-Santos, E.N. Bodunov, L. Pogliani, On the barometric formula, Am. J. Phys. 65 (5) (1997) 404–412.
[23] F. Gallaire, P.T. Brun, Fluid dynamic instabilities: theory and application to pattern forming in complex media, Philos. Trans. R. Soc. A Math. Phys. Eng. Sci. 375 (2093) (2017), 20160155.
[24] F. Boulogne, M.A. Fardin, S. Lerouge, L. Pauchard, F. Giorgiutti-Dauphiné, Suppression of the Rayleigh–Plateau instability on a vertical fibre coated with wormlike micelle solutions, Soft Matter 9 (32) (2013) 7787–7796.